Synthesis C. R. Woof et al. THIEME OPEN ACCESS Special Topic

Catalytic Hydrophosphination of Allenes Using an Iron(II) β-Diketiminate Complex

Callum R. Woof
Thomas G. Linford-Wood
Mary F. Mahon
Ruth L. Webster*

Department of Chemistry, University of Bath, Claverton Down, Bath, BA2 7AY, UK
r.l.webster@bath.ac.uk

Published as part of the Special Topic
Synthetic Advancements Enabled by Phosphorus Redox Chemistry

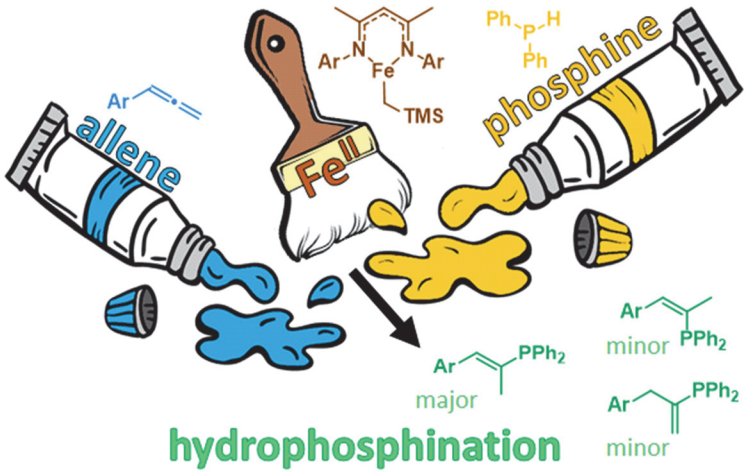

Received: 14.06.2022
Accepted after revision: 14.07.2022
Published online: 18.07.2022 (Accepted Manuscript), 22.08.2022 (Version of Record)
DOI: 10.1055/a-1902-5592; Art ID: SS-2022-06-0290-ST

Abstract A rare study into the catalytic hydrophosphination of allenes is reported. Employing an Fe(II) β-diketiminate pre-catalyst, the reaction of $HPPh_2$ proceeds with a range of aryl- and alkylallenes. For arylallenes the *E*-vinyl product forms as the major species, while the 1,1-disubstituted alkene is formed in a larger ratio than the *Z*-vinyl product (e.g., 6:3:1 as *E*/1,1/*Z*). The use of H_2PPh results in good yields of the 1,1-disubstituted alkene, where the resultant secondary phosphine product does not undergo further reaction. We postulate a catalytic cycle based on spectroscopic data. Employing an $[Fe(salen)]_2$-μ-oxo pre-catalyst leads to phosphine dehydrocoupling rather than hydrophosphination.

Key words iron, homogeneous catalysis, hydrophosphination, allenes, phosphines

Allenes are emerging as a key building block in organic synthesis owing to their unique reactivity, variety of functionalization modes and relative ease of synthesis. Of particular interest in recent years have been routes to forming carbon–heteroatom bonds using allenes as organic substrates. There has been a great deal of interest in the catalytic hydroamination of allenyl substrates,[1] as well as hydroboration[2] and hydrosilylation[3] methods. These reactions generate complex and multi-functional compounds in a straightforward and atom-efficient manner.

Compared to these elements however, there are relatively few studies involving phosphorus-based functionalization of allenes (Scheme 1). This is somewhat surprising given how often the hydrophosphination of styrenes, aryl acetylenes and even heterocumulenes is reported in the literature.[4] These reactions potentially offer new and unusual organophosphorus compounds, as well an atom economical reaction pathway to them. Various routes to and classes of allenylphosphonates have been reported,[5] and these have been shown to be capable of undergoing further intramolecular[6] and intermolecular[7] reactions. Enantioselective hydrophosphinylation has also been reported.[8] In terms of hydrophosphination chemistry, Mitchell initially reported the addition of diphenylphosphine over allenes through radical addition.[9] More recently, rare-earth- and transition-metal-catalyzed methods have been developed. Takaki reported an ytterbium-catalyzed route followed by oxidative work-up leading to phosphine oxide products,[10] while Busacca reported using phosphine-boranes as a P(III) source requiring a stoichiometric equivalent of a metal hydride.[11] In addition, Leung has demonstrated a double hydrophosphination reaction with applications in ligand design.[12] There are also a range of palladium-catalyzed reactions using P(V) sources of phosphorus, including hydrophosphination using pinacol phosphonate,[13] hypophosphorous acid[14] and H-phosphonates.[15] Lu and co-workers have used a catalytic amount of

a tertiary phosphine to undertake [3+2] cycloadditions of allene substrates, forming cyclopentene products.[16] More recently, this transformation was studied in detail by Ofial and co-workers, with vinyl phosphonium intermediates being trapped to allow characterization of the phosphine addition products,[17] the chemoselectivity of which is similar to that obtained from a hydrophosphination reaction.

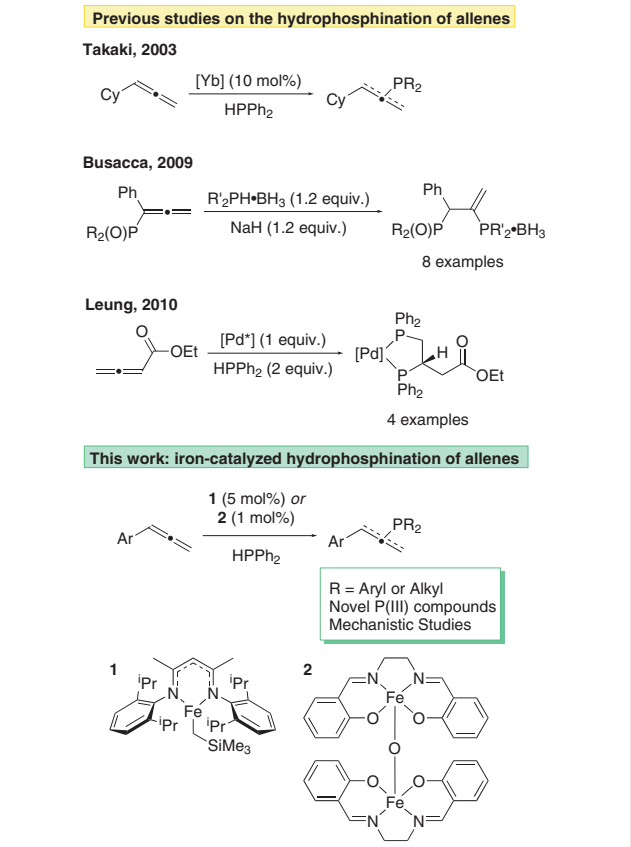

Scheme 1 Previous studies and this work. Herein, we report the hydrophosphination of allenes with diphenylphosphine and other P(III) reagents catalyzed by a β-diketiminate iron complex.

We have previously reported hydrophosphination reactions utilizing alkenes and alkynes catalyzed by various iron complexes,[18] as well as nickel-catalyzed[19] and base-mediated[20] methods. We were interested to see if iron complexes **1** or **2** (see Scheme 1) would be capable catalysts for the hydrophosphination of allenes. This reaction is desirable owing to the sustainability and environmental credentials of iron in catalysis, the high conversion and selectivity reported previously for alkenes and alkynes, and the potential to prepare new phosphorus architectures.

Initial reaction optimization studies were undertaken using phenylallene (**PA**) and diphenylphosphine ($HPPh_2$) as reagents. Based on the wealth of previous studies where **1** is employed as a pre-catalyst, care must be taken when optimizing the hydrophosphination reaction in order to minimize competing phosphine dehydrocoupling (forming P_2Ph_4 and H_2) and allene polymerization reactions. Our initial set of reaction conditions employed 5 mol% of **1**, a 1:1 ratio of **PA**/$HPPh_2$ and generated the terminal *E* isomer **3B** as the major hydrophosphination product, but the major reaction product was P_2Ph_4 (Scheme 2). Performing the reaction at room temperature with **1** led to very low conversion, and at raised temperatures with equimolar amounts of reagents the chemoselectivity towards hydrophosphination is still poor, although it is improved with stirring (see Scheme 2). A drop-off in conversion is observed without stirring, along with a large amount of Ph_4P_2 being produced. Surprisingly, a slight excess of $HPPh_2$ (0.1 mmol excess relative to **PA**) shows a drop-off in overall conversion, but this is predominantly due to the dehydrocoupling pathway being switched off. A further increase in $HPPh_2$ loading (to 1 mmol in total) shows a modest increase in conversion, where more of the unusual 1,1-disubstituted (herein referred to as 'internal') hydrophosphination product **3C** forms. Even with this excess, no doubly-hydrophosphinated products are observed. A change in solvent to CD_2Cl_2 does not alter the hydrophosphination product distribution. In contrast, using a slight excess of **PA** (0.6 mmol **PA**:0.5 mmol $HPPh_2$) leads to high chemoselectivity towards the hydrophosphinated products (51% **3B**, 23% **3C**, 8% **3A**). We observed three distinct products that can be distinguished through both ^{31}P and ^{1}H NMR (see the Supporting Information for full characterization of products). The reaction is reasonably regioselective towards functionalization of the terminal bond over the internal bond (51% vs 23% conversion), and strongly stereoselective towards the *E* isomer over the *Z* isomer (51% vs 8% conversion). The strong *E* selectivity is in-line with the generally *E*- or non-selective catalytic outcomes when preparing these compounds from 1-methyl-1-propyne. It is worth commenting on the conflicting reports of the formation of the *E* or *Z* isomer (**3B** or **3A**) reported in the literature from the reaction of $HPPh_2$ and 1-methyl-1-propyne: Mitchell and Heesche reported (*E*)-diphenyl(1-phenylprop-1-en-2-yl)phosphane (i.e., **3B**) appearing at +6.8 ppm in the ^{31}P NMR spectrum[9] and (*Z*)-diphenyl(1-phenylprop-1-en-2-yl)phosphane (i.e., **3A**) appearing at –14.8 ppm in the ^{31}P NMR spectrum. This regiochemistry/NMR chemical shift has been reported by several others.[10,21] Work from Bookham,[22] which uses diphenylacetylene as a substrate,[23] reports the *Z*-product ((*Z*)-(1,2-diphenylvinyl)diphenylphosphine) at –7.8 ppm and the *E*-product ((*E*)-(1,2-diphenylvinyl)diphenylphosphine) at +8.7 ppm. Bookham's work is cited by Westerhausen as having comparable data to (*E*)-diphenyl(1-phenylprop-1-en-2-yl)phosphane, for which a crystal structure is reported.[24] However, there are conflicting reports in the literature, whereby **3A** is stated to appear at a negative ppm value (approximately –14 ppm) and **3B** is stated to appear at a positive ppm value (approximately +7 ppm).[25] We would expect that a phosphorus atom located *trans* across a dou-

ble bond to a phenyl group might experience greater deshielding than a phosphorus atom located *trans* across a double bond to a proton; coupled with the evidence provided by Westerhausen, we favor **3A** appearing at –13.3 ppm and **3B** appearing at +8.4 ppm in $CDCl_3$. On top of this, although complex, **3A**, **3B** and **3C** display clear coupling in the ^{31}P NMR spectra such that we can assign the signals with reasonable confidence (Figure 1). It is important to note that when mixtures of products form, the 2-dimensional correlation of ^{1}H and ^{31}P NMR spectral data, and thus assignment of the products, is not trivial.

Although [Fe(salen)]$_2$-μ-oxo complex **2** is a highly active pre-catalyst for the hydrophosphination of styrenes and acrylates, it does not perform well in this hydrophosphination reaction. Using **2** instead of **1** under these conditions does not result in the same high chemoselectivity, highlighting the importance of the catalyst structure in reaction control. It is surprising that **2** is a highly competent pre-catalyst for dehydrocoupling $HPPh_2$.

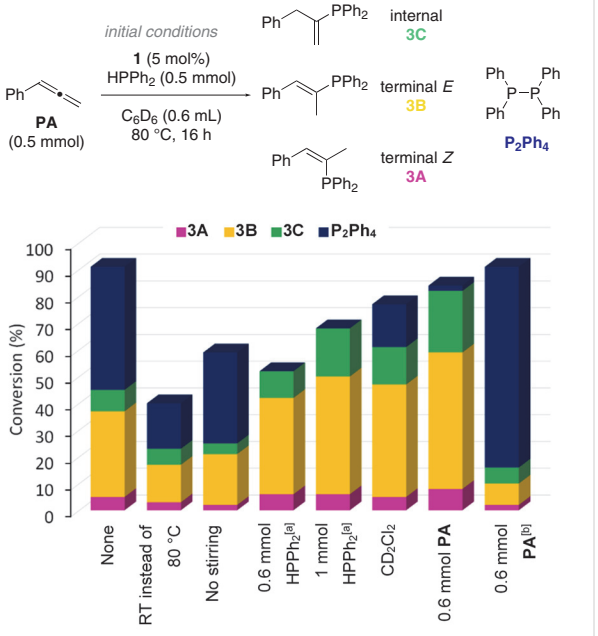

Scheme 2 Optimization of the reaction (deviation from initial conditions listed). Conversions determined by inverse-gated ^{31}P NMR spectroscopy with PPh_3 as an internal standard and reported relative to $HPPh_2$ consumption unless noted. [a] Conversion relative to allene using ^{1}H NMR with 1,3,5-trimethoxybenzene as an internal standard. [b] 1 mol% of **2** used and CH_3CN employed instead of C_6D_6.

We further sought to apply this reactivity to other allene substrates (Figure 2). A range of functionalized arylallenes are tolerated in similar conversions and selectivity to **PA**. Electron-rich substrates give particularly high hydrophosphination conversions, ranging from 74% to 91%; total hydrophosphination conversions of 74% for ***o*-Me-PA** and

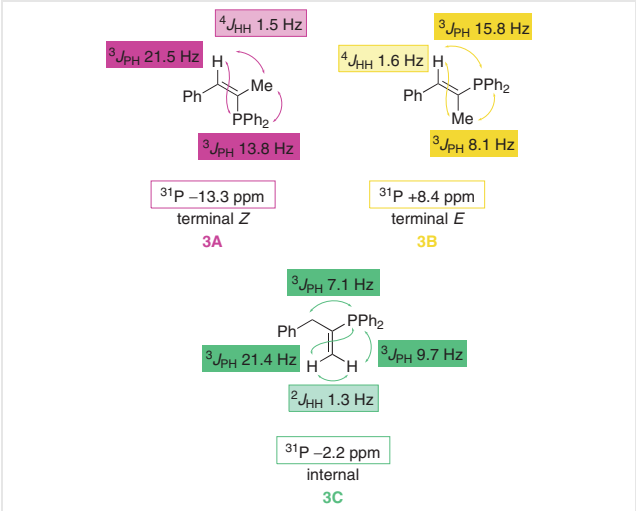

Figure 1 Key coupling interactions observed for **3A**, **3B** and **3C** via ^{31}P and ^{1}H NMR spectroscopy

91% for ***o*-OMe-PA** are observed, which is surprising given the steric hindrance present in these two starting materials and their products. There is a decrease in hydrophosphination conversion for strongly electron-withdrawing ***p*-F-PA**, but this is observed as 4% (**11A**), 54% (**11B**) and 1% (**11C**), so although the overall conversion is modest, the selectivity for **11B** is excellent. For all arylallenes there is a preference for the formation of the terminal *E* isomer over the terminal *Z* and internal isomers, although the specific ratio of the three products does vary. In general, there is a larger quantity of the unusual internal isomer **C** formed when electron-rich **PA** substrates are employed (compare electron-poor substrates ***p*-Cl-PA 9** and ***p*-F-PA 11** to methyl and methoxy substrates **4**–**8**). Using cyclohexylallene (**Cy-A**, **12**) generates five isomeric products (see the Supporting Information) rather than three, although the overall conversion is low at 40%. Hydrophosphination of methoxyallene (**OMe-A**, **13**) yields only the two terminal products, as well as a small amounts of the double hydrophosphination product, but again the conversion is relatively poor.

Several alternative phosphorus reagents were also tested in catalysis with **PA**. $HPCy_2$ is considerably less active than $HPPh_2$ (Table 1, entry 1). Excitingly, reactions with H_2PPh form the internal product **15C** with good selectivity and a good overall yield (entry 2). No double hydrophosphination is observed, even when H_2PPh is used in excess (entry 3). In contrast, H_2PCy does not hydrophosphinate at all under these reaction conditions. In all cases the corresponding P–P-bonded product is not observed. This is likely due to the higher reaction temperature needed (110 to 120 °C) to undertake dehydrocoupling of $HPCy_2$, H_2PPh or H_2PCy with pre-catalyst **1**.[26]

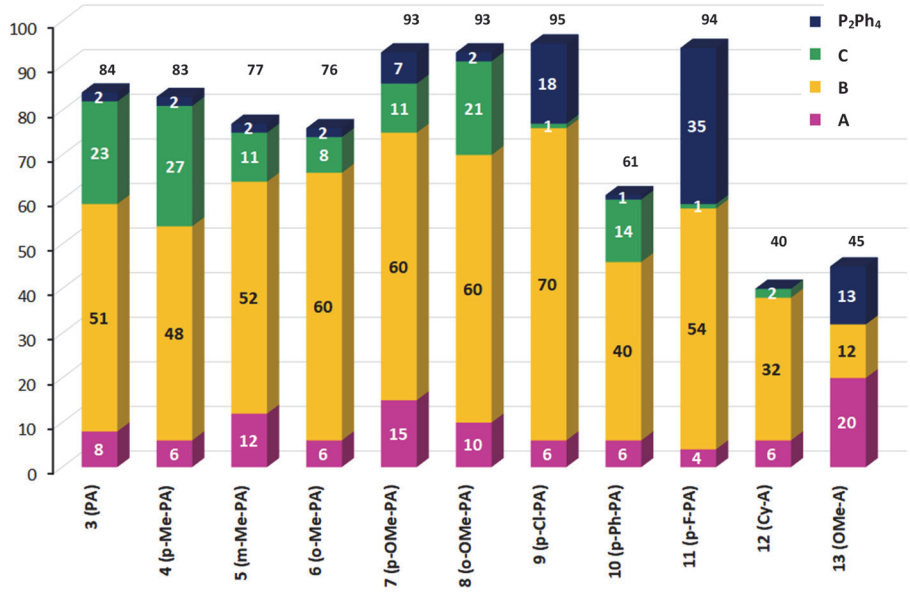

Figure 2 Substrate scope for the hydrophosphination of allenes with $HPPh_2$ using pre-catalyst **1**. Conditions: 0.6 mmol allene, 0.5 mmol $HPPh_2$, 0.025 mmol **1**, 0.6 mL C_6D_6. Conversions determined by inverse-gated ^{31}P NMR spectroscopy with PPh_3 as an internal standard and reported relative to $HPPh_2$. Total conversion shown above each column. See the Supporting Information for further details.

Table 1 Variation of the Phosphorus Reagent[a]

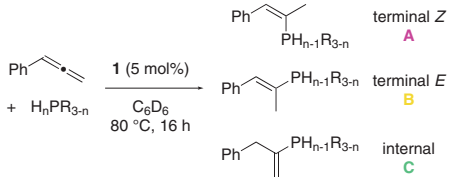

Entry	Substrate (H_nPR_{3-n})	Conversion (%)			
		A	B	C	Total
1	$HPCy_2$ (**14**)	1	5	2	8
2	H_2PPh (**15**)	2	1	62	65
3	H_2PPh (**15**)[b]	2	1	64	67
4	H_2PCy (**16**)	0	0	0	0

[a] Conditions: 0.6 mmol **PA**, 0.5 mmol phosphine, 0.025 mmol **1**, 0.6 mL C_6D_6. Conversions determined by inverse-gated ^{31}P NMR spectroscopy with PPh_3 as an internal standard and reported relative to $HPPh_2$.
[b] 1.0 mmol H_2PPh used; conversion relative to **PA**.

We have previously conducted mechanistic investigations into the hydrophosphination of alkynes using **1** and $HPPh_2$, and the reaction reported herein appears to have similarities. We can rule out nanoparticle involvement through poisoning experiments, while radical-clock reactions appear to confirm the hydrophosphination reaction is not radical-mediated, but the competing dehydrocoupling[26] reaction is likely to be a radical process. The reaction is unaffected by the presence of benzaldehyde, which appears to rule out a nucleophilic phosphorus-based mechanism where we might expect to see reaction with the carbonyl if an intermediate of the form [Fe]–PPh_2 acts as a nucleophile toward the allene, and thus an anionic center is present during the catalytic cycle. When using $DPPh_2$ in the hydrophosphination of **PA** we observe regioselectively monodeuterated products, which are formed in a similar ratio as the reaction with $HPPh_2$ (Scheme 3). This indicates that the hydrophosphination step is direct rather than proceeding through product or substrate rearrangement, or reversible protonolysis steps.

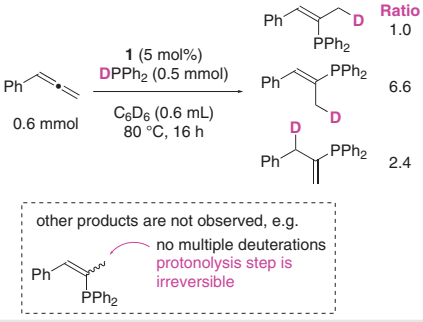

Scheme 3 The use of $DPPh_2$ in the hydrophosphination of **PA**

We propose the initial activation of **1** involves the formation of an iron-phosphido complex by reacting with $HPPh_2$, releasing $Si(Me)_4$, which is observed in the in situ ^1H NMR spectra (Scheme 4). Similar compounds have been previously prepared,[27] although stoichiometric reactions of **1** and $HPPh_2$ lead to only Ph_4P_2 being isolated, which highlights the reactive nature of the iron-phosphido species. The iron-phosphido intermediate can then add across one of the unsaturated carbon–carbon bonds; the regio- and stereoselectivity are determined by the bond added over (and for the terminal products, the face added across). The iron–carbon bond can then be cleaved by protonolysis with a second molecule of $HPPh_2$, generating the hydrophosphinated product. Although the resulting product is unsaturated, it is less amenable to further reactivity, largely due to sterics, preventing double hydrophosphination. We propose that the regiochemistry observed, although clearly driven towards the thermodynamic *E*-product **B**, may have other factors at play. For example, with sterically hindered ***o*-Me-PA** only 8% of **6C** is formed, compared to 27% of **4C** (from ***p*-Me-PA**), so it can be argued in this case that sterics limit the formation of the **C** product, favoring the **B** product (60% of **6B** vs 48% of **4B**). In contrast, this trend is not enacted when we compare ***p*-OMe-PA** to ***o*-OMe-PA**, the same conversion to **7B** and **8B** is observed (60%), but this time a greater conversion to **8C** is observed (21% of **8C** compared to 11% of **7C**); clearly a simple steric argument does not hold true here. However, there may be transient coordination of the *o*-OMe group in the iron-allyl intermediate that benefits **8C**. However, we have not been able to crystallize, or observe by NMR spectroscopy, any long-lived intermediates.

To further prove the likelihood of a catalyst activation event that forms an on-cycle iron-phosphido intermediate, we employed less sterically encumbered β-diketiminate species **1′** in a stoichiometric reaction with $HPPh_2$. Orange crystals of complex **1′·PHPh$_2$** were isolated following reaction at 60 °C for 1 hour and crystallization at –20 °C (Figure 3). Heating **1′·PHPh$_2$** in an attempt to release $SiMe_4$ from the complex only leads to decomposition.

To test the hypothesis that the production of internal product **C** is, in some cases, limited by steric influence from the β-diketiminate ligand, the less sterically demanding pre-catalyst **1′** was employed. Taking **PA**, ***p*-Me-PA**, ***p*-OMe-PA** and ***p*-Cl-PA** as test substrates, we observed an increase in selectivity for **3C**, **4C**, **7C** and **9C** (Table 2).

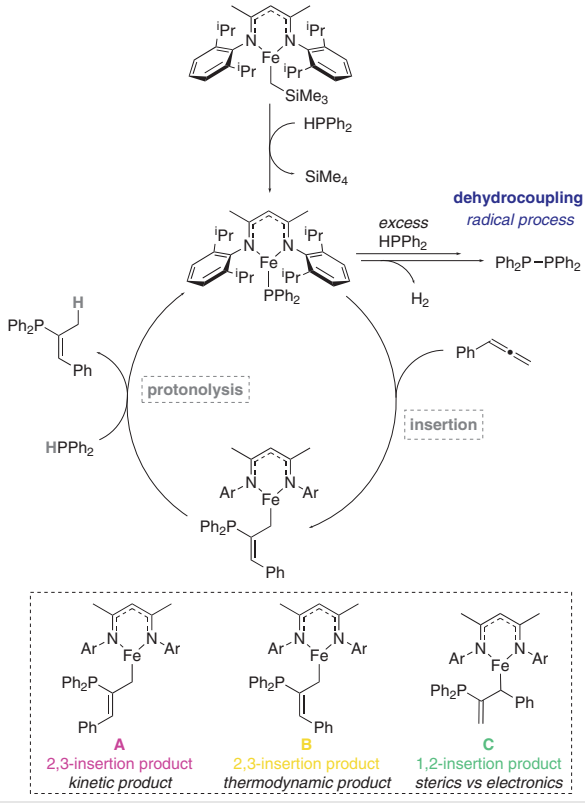

Scheme 4 Proposed catalytic cycle

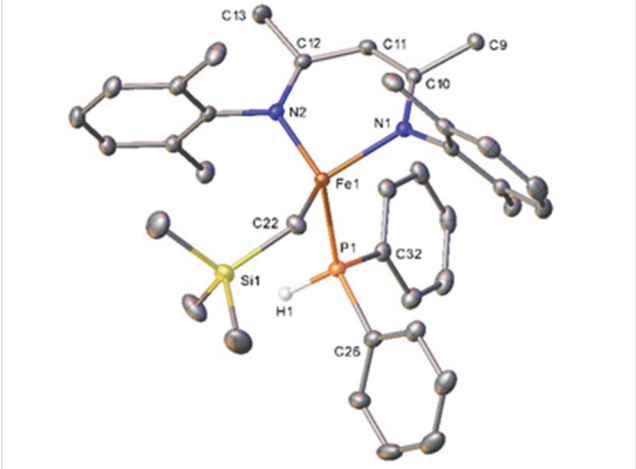

Figure 3 Crystal structure of **1′·PHPh$_2$**. With the exception of H1, all hydrogen atoms have been removed for clarity. Ellipsoids displayed at 30% probability. Selected bond metrics: Fe1–P1, 2.4937(4) Å; Fe1–C22, 2.0588(15) Å; N2–Fe1–N1, 91.71(5)°; C22–Fe1–P1, 103.02(5)°.

Table 2 Product Distribution Using Pre-catalyst **1¢**

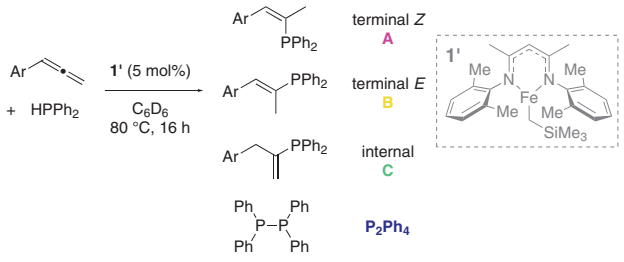

Entry	Substrate	Conversion (%)			
		A	B	C	P_2Ph_4
1	**PA** (**3**)	trace	86	11	trace
2	***p*-Me-PA** (**4**)	9	15	60	trace
3	***p*-OMe-PA** (**7**)	5	77	13	3
4	***p*-Cl-PA** (**9**)	trace	13	79	trace

Other factors beyond sterics and even electronics are at play: the conversion into **4C** and **9C** (Table 2, entries 2 and 4) are dramatically improved when using **1′** compared to pre-catalyst **1** (11% of **4C** and 1% of **9C**, see Figure 2). However, in the presence of **1′**, both **PA** and ***p*-OMe-PA** show an improvement in selectivity for products **3B** and **7B** (86% and 77% using **1′** compared to 51% and 60% using **1**, compare Table 2, entries 1 and 3 with Figure 2).

In summary, we have reported the hydrophosphination of allene substrates using an iron(II) β-diketiminate pre-catalyst and $HPPh_2$ as a phosphorus source. This reaction tolerates a range of aryl and non-arylallenes, with high levels of selectivity for the *E*-vinyl product. The reaction proceeds well with H_2PPh, generating the 1,1-disubstituted ('internal') alkene product with no evidence for over functionalization of the resultant P–H bond. A deuterium-labelling study showed clean transfer of the deuterium from $DPPh_2$, with no evidence for multiple deuterations, indicating an irreversible proton transfer step. This, coupled with the lack of telomerization or reaction with benzaldehyde, thus ruling out a nucleophilic attack-type mechanism, means that we have been able to postulate a reaction that proceeds via insertion of an allene into an iron-phosphido intermediate followed by protonolysis and regeneration of the iron-phosphido complex. Interestingly, we also report on the ability of an iron(III)-μ-oxo complex, previously reported as a highly active pre-catalyst for the hydrophosphination of styrenes, to undertake dehydrocoupling to form P_2Ph_4 rather than hydrophosphination of allenes.

Reagents were purchased from Sigma-Aldrich or Acros, with the exception of pentane and bromoform (Fisher). Solvents used in synthesis/reactions were dried with sodium/benzophenone and distilled before use. NMR data were collected on 300, 400 or 500 MHz Bruker or Agilent machines as stated. ^1H, ^{13}C and ^2H chemical shifts were referenced to residual solvent peaks, while ^{31}P and $^{31}P\{^1H\}$ NMR were referenced to PPh_3 (5.3 ppm). Mass spectrometry data was obtained using an Agilent 6545 Q-Tof LC/MS spectrometer. FTIR data was collected on a PerkinElmer Spectrum 100 FT-IR Spectrometer. All manipulations were carried out under an inert atmosphere using standard Schlenk/glove box techniques unless stated.

Crystallographic Data for 1¢·$PHPh_2$ (Using Cu-Ka Radiation)

All experiments were conducted at 150 K, solved using SHELXS and refined using SHELXL via the Olex2 interface. Crystallographic data for **1′** have been deposited with the Cambridge Crystallographic Data Centre. CCDC 2178990 (**1′·$PHPh_2$**) contains the supplementary crystallographic data for this paper. The data can be obtained free of charge from The Cambridge Crystallographic Data Centre via www.ccdc.cam.ac.uk/structures.

Hydrophosphination; General Procedure

Experiments were performed under an argon atmosphere in an M-Braun glove box. To a flame-dried J-Young ampoule of approximately 20 mL volume was added the required pre-catalyst (0.025 mmol, 5 mol%). To this was added the required allene (0.6 mmol) and phosphine (0.5 mmol). The ampoule was then sealed and heated, with stirring, for the times and conditions reported.

Spectroscopic conversions were determined by decanting the reaction mixture into a J-Young NMR tube at the end of the reaction and calculating the conversion by inverse-gated ^{31}P NMR using PPh_3 as an internal standard. The solvent was then removed from the reaction, and the hydrophosphination products were isolated through column chromatography (silica gel, 80% petroleum ether/20% DCM as the eluent) under air. For the majority of products this work-up yields the phosphine products, although a small amount of phosphine oxides are observed in ^{31}P and ^1H NMR. Some reactions generated products that oxidize rapidly in air – these were isolated from the catalyst by means of filtration through a silica plug under an argon atmosphere using 100% pentane as the eluent. These are noted in the product characterization section.

See the Supporting Information for analysis data and spectra.

Conflict of Interest

The authors declare no conflict of interest.

Funding Information

The Engineering and Physical Sciences Research Council (EPSRC) and the EPSRC Centre for Doctoral Training in Catalysis (Ph.D. studentships awarded to C.R.W. and T.G.L.-W.) are thanked for funding.

Acknowledgment

The authors would like to thank Jonathan Nevett for some preliminary optimizations.

Supporting Information

Supporting information for this article is available online at https://doi.org/10.1055/a-1902-5592.

References

(1) (a) Perego, L. A.; Blieck, R.; Groué, A.; Monnier, F.; Taillefer, M.; Ciofini, I.; Grimaud, L. *ACS Catal.* **2017**, *7*, 4253. (b) Kinder, R. E.; Zhang, Z.; Widenhoefer, R. A. *Org. Lett.* **2008**, *10*, 3157. (c) Michon, C.; Medina, F.; Abadie, M.-A.; Agbossou-Niedercorn, F. *Organometallics* **2013**, *32*, 5589. (d) Ayinla, R. O.; Schafer, L. L. *Dalton Trans.* **2011**, *40*, 7769. (e) Xu, K.; Wang, Y.-H.; Khakyzadeh, V.; Breit, B. *Chem. Sci.* **2016**, *7*, 3313.

(2) (a) Kister, J.; DeBaillie, A. C.; Lira, R.; Roush, W. R. *J. Am. Chem. Soc.* **2009**, *131*, 14174. (b) Nagashima, Y.; Sasaki, K.; Suto, T.; Sato, T.; Chida, N. *Chem. Asian J.* **2018**, *13*, 1024. (c) Li, C.; Yang, Z.; Wang, L.; Guo, Y.; Huang, Z.; Ma, S. *Angew. Chem. Int. Ed.* **2020**, *59*, 6278. (d) Semba, K.; Shinomiya, M.; Fujihara, T.; Terao, J.; Tsuji, Y. *Chem. Eur. J.* **2013**, *19*, 7125. (e) Yasunori, Y.; Ryou, F.; Akihiko, Y.; Norio, M. *Chem. Lett.* **1999**, *28*, 1069.

(3) (a) Tafazolian, H.; Schmidt, J. A. R. *Chem. Commun.* **2015**, *51*, 5943. (b) Kidonakis, M.; Stratakis, M. *Org. Lett.* **2015**, *17*, 4538. (c) Wang, C.; Teo, W. J.; Ge, S. *Nat. Commun.* **2017**, *8*, 2258. (d) Cai, Y.; Zhao, W.; Wang, S.; Liang, Y.; Yao, Z.-J. *Org. Lett.* **2019**, *21*, 9836. (e) Jiang, Y.-N.; Zeng, J.-H.; Yang, Y.; Liu, Z.-K.; Chen, J.-J.; Li, D.-C.; Chen, L.; Zhan, Z.-P. *Chem. Commun.* **2020**, *56*, 1597.

(4) (a) Zagidullin, A. A.; Sakhapov, I. F.; Miluykov, V. A.; Yakhvarov, D. G. *Molecules* **2021**, *26*, 5283. (b) Seah, J. W. K.; Teo, R. H. X.; Leung, P. H. *Dalton Trans.* **2021**, *50*, 16909. (c) Huke, C. D.; Kays, D. L. *Hydrofunctionalization Reactions of Heterocumulenes: Formation of C–X (X = B, N, O, P, S and Si) Bonds by Homogeneous Metal Catalysts*, In *Advances in Organometallic Chemistry, Vol. 75*; Perez, P. J., Ed.; Academic Press: Cambridge, **2021**, 1–54. (d) Beletskaya, I. P.; Najera, C.; Yus, M. *Russ. Chem. Rev.* **2021**, *90*, 70. (e) Banerjee, I.; Panda, T. K. *Org. Biomol. Chem.* **2021**, *19*, 6571. (f) Li, Y. Y.; Cheng, Y. H.; Shan, C. H.; Zhang, J.; Xu, D. D.; Bai, R. P.; Au, L. B.; Lan, Y. *Chin. J. Org. Chem.* **2018**, *38*, 1885. (g) Uhl, W.; Keweloh, L.; Hepp, A.; Stegemann, F.; Layh, M.; Bergander, K. *Z. Anorg. Allg. Chem.* **2017**, *643*, 1978. (h) Gusarova, N. K.; Chernysheva, N. A.; Trofimov, B. A. *Synthesis* **2017**, *49*, 4783. (i) Bezzenine-Lafollee, S.; Gil, R.; Prim, D.; Hannedouche, J. *Molecules* **2017**, *22*, 1901.

(5) (a) Chakravarty, M.; Bhuvan Kumar, N. N.; Sajna, K. V.; Kumara Swamy, K. C. *Eur. J. Org. Chem.* **2008**, 4500. (b) Kalek, M.; Stawinski, J. *Adv. Synth. Catal.* **2011**, *353*, 1741. (c) Chakravarty, M.; Kumara Swamy, K. C. *J. Org. Chem.* **2006**, *71*, 9128.

(6) Shen, R.; Yang, J.; Zhang, M.; Han, L.-B. *Adv. Synth. Catal.* **2017**, *359*, 3626.

(7) Fourgeaud, P.; Daydé, B.; Volle, J.-N.; Vors, J.-P.; Van der Lee, A.; Pirat, J.-L.; Virieux, D. *Org. Lett.* **2011**, *13*, 5076.

(8) Yang, Z.; Wang, J. *Angew. Chem. Int. Ed.* **2021**, *60*, 27288.

(9) Mitchell, T. N.; Heesche, K. *J. Organomet. Chem.* **1991**, *409*, 163.

(10) Takaki, K.; Koshoji, G.; Komeyama, K.; Takeda, M.; Shishido, T.; Kitani, A.; Takehira, K. *J. Org. Chem.* **2003**, *68*, 6554.

(11) Busacca, C. A.; Farber, E.; DeYoung, J.; Campbell, S.; Gonnella, N. C.; Grinberg, N.; Haddad, N.; Lee, H.; Ma, S.; Reeves, D.; Shen, S.; Senanayake, C. H. *Org. Lett.* **2009**, *11*, 5594.

(12) Huang, Y.; Pullarkat, S. A.; Yuan, M.; Ding, Y.; Li, Y.; Leung, P.-H. *Organometallics* **2010**, *29*, 536.

(13) Zhao, C.-Q.; Han, L.-B.; Tanaka, M. *Organometallics* **2000**, *19*, 4196.

(14) Bravo-Altamirano, K.; Abrunhosa-Thomas, I.; Montchamp, J.-L. *J. Org. Chem.* **2008**, *73*, 2292.

(15) Hu, S.; Sun, W.; Chen, J.; Li, S.; Zhao, R.; Xu, P.; Gao, Y.; Zhao, Y. *Chem. Commun.* **2021**, *57*, 339.

(16) Zhang, C.; Lu, X. *J. Org. Chem.* **1995**, *60*, 2906.

(17) An, F.; Jangra, H.; Wei, Y.; Shi, M.; Zipse, H.; Ofial, A. R. *Chem. Commun.* **2022**, *58*, 3358.

(18) (a) Gallagher, K. J.; Webster, R. L. *Chem. Commun.* **2014**, *50*, 12109. (b) Espinal-Viguri, M.; King, A. K.; Lowe, J. P.; Mahon, M. F.; Webster, R. L. *ACS Catal.* **2016**, *6*, 7892. (c) Gallagher, K. J.; Espinal-Viguri, M.; Mahon, M. F.; Webster, R. L. *Adv. Synth. Catal.* **2016**, *358*, 2460.

(19) Webster, R. *Inorganics* **2018**, *6*, 120.

(20) Coles, N. T.; Mahon, M. F.; Webster, R. L. *Chem. Commun.* **2018**, *54*, 10443.

(21) Blackaby, W. J. M.; Neale, S. E.; Isaac, C. J.; Sabater, S.; Macgregor, S. A.; Whittlesey, M. K. *ChemCatChem* **2019**, *11*, 1893.

(22) Bookham, J. L.; McFarlane, W.; Thornton-Pett, M.; Jones, S. *J. Chem. Soc., Dalton Trans.* **1990**, 3621.

(23) Bookham, J. L.; Smithies, D. M.; Wright, A.; Thornton-Pett, M.; McFarlane, W. *J. Chem. Soc., Dalton Trans.* **1998**, 811.

(24) Al-Shboul, T. M. A.; Pálfi, V. K.; Yu, L.; Kretschmer, R.; Wimmer, K.; Fischer, R.; Görls, H.; Reiher, M.; Westerhausen, M. *J. Organomet. Chem.* **2011**, *696*, 216.

(25) (a) Hayashi, M.; Matsuura, Y.; Watanabe, Y. *J. Org. Chem.* **2006**, *71*, 9248. (b) Hu, H.; Cui, C. *Organometallics* **2012**, *31*, 1208. (c) Moglie, Y.; González-Soria, M. J.; Martín-García, I.; Radivoy, G.; Alonso, F. *Green Chem.* **2016**, *18*, 4896. (d) Pollard, V. A.; Young, A.; McLellan, R.; Kennedy, A. R.; Tuttle, T.; Mulvey, R. E. *Angew. Chem. Int. Ed.* **2019**, *58*, 12291. (e) Barrett, A. N.; Sanderson, H. J.; Mahon, M. F.; Webster, R. L. *Chem. Commun.* **2020**, *56*, 13623. (f) Basiouny, M. M. I.; Dollard, D. A.; Schmidt, J. A. R. *ACS Catal.* **2019**, *9*, 7143. (g) Novas, B. T.; Bange, C. A.; Waterman, R. *Eur. J. Inorg. Chem* **2019**, 1640.

(26) King, A. K.; Buchard, A.; Mahon, M. F.; Webster, R. L. *Chem. Eur. J.* **2015**, *21*, 15960.

(27) Kaniewska, K.; Dragulescu-Andrasi, A.; Ponikiewski, Ł.; Pikies, J.; Stoian, S. A.; Grubba, R. *Eur. J. Inorg Chem.* **2018**, 4298.